

Article

Ammonia–Mechanical Pretreatment of Wheat Straw for the Production of Lactic Acid and High-Quality Lignin

Yulian Cao ^{1,2}, Haifeng Liu ², Junqiang Shan ², Baijun Sun ³, Yanjun Chen ², Lei Ji ², Xingxiang Ji ¹, Jian Wang ³, Chenjie Zhu ^{2,*}  and Hanjie Ying ²

¹ State Key Laboratory of Biobased Material and Green Papermaking, Qilu University of Technology (Shandong Academy of Sciences), Jinan 250353, China

² College of Biotechnology and Pharmaceutical Engineering, Nanjing Tech University, Nanjing 211816, China

³ Hangzhong Dehong Technology Co., Ltd., Hangzhou 310015, China

* Correspondence: zhucj@njtech.edu.cn; Tel.: +86-15261868731

Abstract: In this study, wheat straw was fractionated into carbohydrates (cellulose and hemicellulose) by ammonia–mechanical pretreatment for L-lactic acid fermentation. Under optimal conditions (aqueous ammonia concentration: 19% *w/w*, liquid–solid ratio: 2.1:1 *w/w*, holding time: 4.80 h), the delignification was more than 60%. After enzymatic hydrolysis, the maximum conversions of cellulose and hemicellulose were 92.5% and 83.4% based on the pretreatment residue, respectively. The wheat straw hydrolysate was used to produce L-lactic acid with *Thermoanaerobacter* sp. DH-217G, which obtained a yield of 88.6% and an optical purity of 99.2%. The ammonia–mechanical pretreatment is an economical method for the production of fermentable monosaccharide, providing potential for further downstream high value-added applications.

Keywords: wheat straw; ammonia–mechanical pretreatment; enzymatic hydrolysis; L-lactic acid fermentation; lignin



Citation: Cao, Y.; Liu, H.; Shan, J.; Sun, B.; Chen, Y.; Ji, L.; Ji, X.; Wang, J.; Zhu, C.; Ying, H. Ammonia–Mechanical Pretreatment of Wheat Straw for the Production of Lactic Acid and High-Quality Lignin. *Fermentation* **2023**, *9*, 177. <https://doi.org/10.3390/fermentation9020177>

Academic Editor: Xiaoqing Lin

Received: 19 January 2023

Revised: 10 February 2023

Accepted: 13 February 2023

Published: 15 February 2023



Copyright: © 2023 by the authors. Licensee MDPI, Basel, Switzerland. This article is an open access article distributed under the terms and conditions of the Creative Commons Attribution (CC BY) license (<https://creativecommons.org/licenses/by/4.0/>).

1. Introduction

Lactic acid is not only an important monomer for the synthesis of biodegradable plastic polylactic acid (PLA), but it is also widely used in the food, medical, pharmaceutical and materials fields [1]. According to the report in [2], the global lactic acid market has reached 1845.00 kilotons in 2022 from 750.00 kilotons in 2017, and the global lactic acid market sizes are expected to grow at an annual growth rate of 12.8% from 2020 to reach USD 2.1 billion by 2025. Currently, both D-/L-lactic acid are produced from crop starch feedstock through microbial fermentation. In view of the cost of using pure sugar and the issue of “food and land competition”, the exploration of using non-food feedstock to supplement or replace food crop starch for production of lactic acid is highly desirable [3,4].

As an abundant, low-cost source of non-food biomass, lignocellulose is a promising candidate for lactic acid fermentation [5]. However, the recalcitrant, complex, and heterogeneous structure and composition of lignocellulosic raw materials make them difficult to use directly as a source for biochemical transformation [6]. Hence, the development of an efficient pretreatment technology for the deconstruction of lignocellulose is crucially important. Numerous strategies such as physical (milling, microwave, ultrasound, and extrusion, etc.), chemical (acid, alkali, organic solvents, ionic liquids, and deep eutectic solvents, etc.), biological (fungi, bacteria, and archaea, etc.), and physicochemical (hot water, steam explosion, ammonia-based, wet oxidation, and carbon dioxide explosion, etc.) methods have been studied and are still in development with varying levels of success; furthermore, the chemical pretreatment was commonly employed in many pilot and demonstration plants because it is ideal for materials with low lignin content [7–9]. Among them, alkali pretreatment was an effective targeting-lignin method for lignin removal or modification, which could break the interlinks between lignin and hemicellulose [10]. Meanwhile, it

usually causes swelling of the biomass, thus increasing enzymatic digestibility and improving saccharification. However, this method often involves saline wastewater requiring further treatment, which leads to additional disposal cost and environmental risk [11]. To address this problem, we developed organic amine [12] or hydrazine hydrate [13] as the alkali catalyst for pretreatment. However, the high cost of these catalysts can hardly meet the requirements of commercial applications. Thus, in this study, we try to use cheaper aqueous ammonia to reduce process costs. However, reported pretreatment methods by using aqueous ammonia for cooking or soaking still have several drawbacks from a practical point of view, such as low efficiency of batch processing, high energy consumption at elevated temperatures, prolonged pretreatment cycles, safety issues under intense pressure and ammonia recovery [14–16]. Therefore, overcoming these shortcomings was the focus of this investigation.

Recently, extrusion was emerged as an attractive process for the pretreatment of lignocellulosic biomass due to its continuous and high processing capacity, low energy consumption, short residence time, and safety profile [17]. Extrusion promotes structural changes in lignocellulose through shearing, mixing, and heating, which give some particular degree of lignocellulose destruction. The mechanical force can lead to an increase in porosity and specific surface area of lignocellulose, enhancing the accessibility for enzymes [18]. Compared to the pure extrusion pretreatment, catalytic extrusion pretreatment, or combined with the other pretreatment, has proven to be a more efficient method [19–21], in view of the issues derived from acid catalytic extrusion pretreatment such as generating inhibitors, equipment corrosion problems [22,23]. In this study, we reported a novel, green, and effective pretreatment technique by combining the advantages of aqueous ammonia catalysis and twin-screw extrusion process intensification in one integration process for the pretreatment of wheat straw. The pretreatment residue was enzyme-hydrolyzed to ferment lactic acid (Figure 1). The effect of ammonia–mechanical pretreatment was investigated thoroughly by analyzing the physical and chemical characteristic variations in wheat straw before and after pretreatment. Furthermore, the produced lignin was also characterized to evaluate its downstream applications.

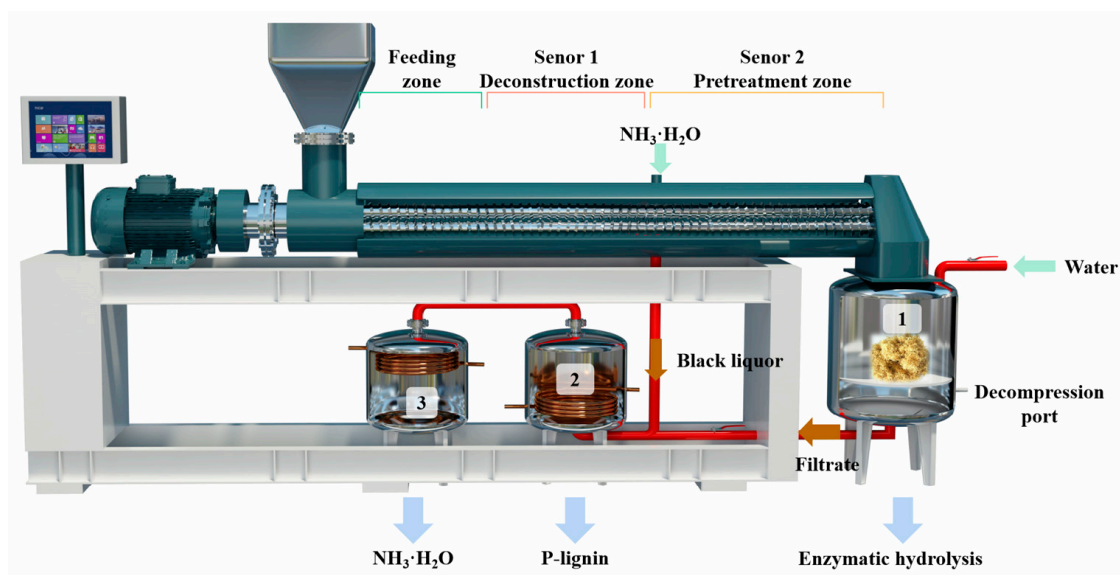


Figure 1. One integration process for the ammonia–mechanical pretreatment of wheat straw: 1. seal pot for heat preservation; 2. evaporation chambers; 3. condensation chambers.

2. Materials and Methods

2.1. Materials

Wheat straw was obtained from a local farmer in Nanyang, Henan, China. Aqueous ammonia ($\text{NH}_3 \cdot \text{H}_2\text{O}$, 25% *w/w*) was purchased from Maclean (Shanghai, China). Cellulase

(CTec 2) with an enzyme activity of 260 FPU/mL (filter paper unit) was obtained from Tianguan Co., Ltd. (Nanyang, China). *Thermoanaerobacter* sp. DH-217G was obtained from Hangzhong Dehong Technology Co., Ltd. (Hangzhou, China). The milled wood lignin (MWL) was isolated from the wheat straw by Björkman's method [24,25]. The dry wheat straw was milled in a planetary ball mill at 450 r/min for 5 h and then extracted by a mixture of 1,4-dioxane and water (96:4, *v:v*) for 48 h. The crude MWL was obtained by adjusting the pH of the filtrate to 2.0, which was purified by dissolving it in a mixture of acetic acid and water (90:10, *v:v*) and dropping the dissolved solution into cold water. Then, the precipitated lignin was centrifuged and freeze-dried. It was further purified by dissolving it in a mixture of 1,2-dichloroethane and ethanol (2:1, *v:v*). Then, the lignin solution was added dropwise into anhydrous ethyl ether. The pure MWL was obtained by centrifugation and was vacuum oven-dried. To facilitate understanding, in this study, pretreatment residue stands for the sample after pretreatment, and enzymatic hydrolysis residue stands for the residue after enzymatic hydrolysis.

2.2. Pretreatment of Biomass

The ammonia–mechanical pretreatment experiments were carried out in the twin-screw extruder (Figure 1). The wheat straw (20 kg on a dry basis) was chopped into 3–5 cm to feed the screw, and the prepared aqueous ammonia of different concentrations was added into the twin-screw extruder for the pretreatment (Section 2 with adjusting the liquid–solid ratio). The parameters of the twin-screw extruder during the experiments were as follows: diameter, 34 mm; speed, 200 r/min; feed rate, 20 kg/h; operating temperature, about 373 K. After pretreatment, the pretreatment residue was placed in the seal pot for heat preservation and then washed with water and separated by filtration. The obtained pretreatment residue was used for the composition analysis and enzymatic hydrolysis. The filtrate and black liquor, through the combined action of evaporation and condensation, chambers recovered the aqueous ammonia. Water was added and the pH was adjusted to 2 by sulfuric acid to obtain the precipitated lignin. It was then spray dried (Spray dryer, SP-1500) and named P-lignin. The purity of P-lignin was assessed by the Klason method with 93.26%.

2.3. Enzymatic Hydrolysis of Biomass

Wheat straw or pretreatment residue (1 g) was added to 20 mL sodium citrate buffer solution (0.05 mol/L, pH 5.0). Enzymatic hydrolysis was performed with cellulase (20 FPU/g dry pretreatment residue) at 323.15 K with an agitation speed of 150 rpm on an insulation shaker for 48 h. Periodically, 50 μ L supernatant was taken, and the sugar concentration was measured during enzymatic hydrolysis. The conversion rate of carbohydrates was used as the following equation:

$$Y_{Cellulose}(\%) = (Glu \times 0.9) / M_{Cellulose} \quad (1)$$

$$Y_{HemiCellulose}(\%) = (Glu \times 0.9) / M_{Hemicellulose} \quad (2)$$

$$Y_{Sugars}(\%) = m_{Sugars} / M_{Sugars} \quad (3)$$

where $Y_{Cellulose}$ and $Y_{Hemicellulose}$ are cellulose and hemicellulose conversion rate, Glu and Xyl are glucose (g) and xylose (g) in the hydrolysate, $M_{Cellulose}$ and $M_{Hemicellulose}$ are the weight of biomass (g), the value of 0.9 was the conversion factor between glucose and cellulose, and the value of 0.88 was the conversion factor between xylose and hemicellulose. Y_{Sugars} is calculated as the total mass of sugars released from treated and untreated dry biomass, m_{Sugars} is all sugars(g) in the hydrolysate, and M_{Sugars} is the sugars of biomass added to enzymatic hydrolysis.

2.4. L-Lactic Acid Fermentation

Thermoanaerobacter sp. DH-217G was grown anaerobically with nitrogen for 18–24 h in the seed medium (including the following (g/L): glucose 30, beef extract 2, $(NH_4)_2SO_4$

2.75, NaCl 0.1, MgSO₄·7H₂O 0.7, CaCO₃ 10) at 328.15 K. The culture was transferred to 20 times of L-lactic acid production medium, (including the following (g/L): beef extract 5, (NH₄)₂HPO₄ 1, (NH₄)₂SO₄ 2.75, NaCl 0.1, MgSO₄·7H₂O 0.7, CaCl₂·2H₂O 0.25, and K₂HPO₄ 0.35) with wheat straw hydrolysate (about 90 g/L total sugar) or about 90 g/L mixture pure sugar as a carbon source, for fermentation. The pH was adjusted to 6.8 by Ca(OH)₂, and the medium was sterilized at 394.15 K for 20 min. The sugars were cold sterilized by a 0.22 mm filter membrane. Ca(OH)₂ was used to modulate the fermentation process. The D/L chiral purity of lactic acid was assayed by a Megazyme D-/L-lactic acid kit (Megazyme International Ireland, Bray, Wicklow, Ireland).

2.5. Component Analysis of Biomass and Fermentation Analysis

The composition of wheat straw or pretreatment residues was analyzed by acid hydrolysis [26]. The concentrations of sugars and L-lactic acid were analyzed by high-performance liquid chromatography (HPLC) (Waters 1525-2414) with an Aminex HPX-87H column (Bio-Rad, Hercules, CA, USA) and a refractive index detector (RID). There was a flow rate of 0.6 mL/min with 5 mM H₂SO₄ as the mobile phase. The recovery of carbohydrates and delignification used the following equation:

$$CR(\%) = (DWP \times CCP) / (DWB \times CCR) \times 100\% \quad (4)$$

$$HR(\%) = (DWP \times CHP) / (DWB \times CHR) \times 100\% \quad (5)$$

$$DL(\%) = 1 - (DWP \times CLP) / (DWB \times CLR) \times 100\% \quad (6)$$

where *CR* and *HR* are cellulose and hemicellulose recovery, and *DL* is the delignification. *DWP* and *DWB* are the dry weight of pretreatment residues and dry weight of biomass fed to pretreatment. *CCP*, *CHP*, and *CLP* are the cellulose, hemicellulose, and lignin content of pretreatment residues. *CCR*, *CHR*, and *CLR* are the cellulose, hemicellulose, and lignin content of raw.

2.6. Characterization of Wheat Straw and Lignin

2.6.1. Microstructure Analysis

The samples were freeze-dried by a freeze dryer (LABCONCO, 2.5 Free Zone, Kansas, Missouri, USA), then surface-sprayed with gold, which was performed with an E-1010 nozzle for 20 s and examined by scanning electron microscope (SEM) (FEI Quanta 200 FEG SEM at 2 kV).

The crystalline structure of wheat straw and pretreatment residues were determined by X-ray diffraction (XRD) (Rigaku ultima IV, Tokyo, Japan), which was scanned from 10° to 40° at a speed of 5°/min. The crystallinity index (*CrI*) was calculated by Equation (7):

$$CrI(\%) = (I_{002} - I_{am}) / I_{002} \times 100\% \quad (7)$$

where *I*₀₀₂ is the spectral intensity for the crystalline portion of biomass at 2θ of 22.5°, and *I*_{am} is the spectral intensity for the amorphous portion of biomass at 2θ of 18.7°.

2.6.2. Ultimate Analysis

The C, H, N, and S of lignin samples were performed by a Carbograph Autoanalyzer (Fison Carlo Erba EA 1110, Thermo Flash & Carlo Erba Analyzers, Marlton, NJ, USA).

2.6.3. Fourier Transform Infrared (FTIR) Spectroscopy

Fourier transform infrared (FTIR) analysis of lignin samples was performed by a TENSOR27 (Bruker, Leipzig, Germany) which was scanned from 4000 to 500 cm⁻¹, at a resolution of 2 cm⁻¹, with 32 scans per sample.

2.6.4. Two-dimensional ^1H - ^{13}C Heteronuclear Single Quantum Coherence (HSQC) NMR Spectroscopy

Two-dimensional HSQC NMR spectra were acquired on a Bruker AVANCE 400 MHz spectrometer, and about 90 mg of lignin samples was dissolved in 0.5 mL DMSO- d_6 . ^1H : spectral width 5000 Hz, sample size 1024, relaxation time 1.5 s, accumulation 64 times; ^{13}C : spectral width 18,000 Hz, sample size 256, hydrocarbon coupling constant 145 Hz [27].

2.6.5. The Radical Scavenging Activity of Lignin

The radical scavenging activity of lignin samples was performed by a DPPH (2,2-diphenyl-1-picrylhydrazyl) kit (Shanghai Acme Biochemical Co., Ltd., Shanghai, China). The results were expressed as *TRAS%* (radical scavenging activity) and calculated based on the following equation:

$$\text{TRAS}\% = \left\{ [A_0 - (A_{\text{Sample}} - A_{\text{Contrast}})] \right\} \times 100\% \quad (8)$$

where A_0 is the absorbance of the bank that does not have a lignin sample, A_{Sample} is the absorbance of the lignin sample, and A_{Contrast} is the absorbance of the contrast.

2.7. Experimental Design and Statistical Analysis

A response surface methodology (RSM) based on Box–Behnken design (BBD) was applied to study the effect of the process, using statistical software (Design expert 10.0.1, Stat-Ease, Inc, Minneapolis, MI, USA). The independent variables were: X_1 , aqueous ammonia concentration (5–25%, *w/w*); X_2 , liquid–solid ratio (1:1–3:1 (*w/w*)); X_3 , holding time (2–6 h). The BBD design was created for 17 experiments with five replications at the center point, as shown in Table S1. The independent variables and their interactions through the regression analysis were optimized, and the second-order polynomial model was fit with the following equation:

$$Y = \beta_0 + \sum_{i=1}^3 \beta_i X_i + \sum_{i=1}^3 \beta_{ii} X_i^2 + \sum_{i<j}^3 X_i X_j \quad (9)$$

where Y is the cellulose or hemicellulose conversion at the end of enzymatic hydrolysis, β_0 is the constant, and β_i , β_{ii} , and β_{ij} are the linear, interaction, and quadratic coefficients, respectively. X_i and X_j are the independent variables (i and j range from 1 to k , $k = 3$).

Analysis of variance (ANOVA) was conducted to determine the significance of the regression coefficients and goodness of fit. The coefficient of determination (R^2) showed a relationship with the experimental and predicted values, and the individual effects of the independent variables on the responses were illustrated by the three-dimensional surface plots. The factor has significant differences when $p < 0.05$.

3. Results and Discussion

3.1. The Ammonia–Mechanical Pretreatment Process and Enzymatic Hydrolysis of Wheat Straw

The twin-screw extruder consists of three zones: the feeding zone, the deconstruction zone, and the pretreatment zone by different screw pitch lengths (Figures 1 and S1). The feeding zone consists of several forward feed screw elements that act as drivers to transport solid biomass to the deconstruction zone. The biomass interacts with the reverse-conveying elements in the deconstruction zone to achieve a change in physical properties. The chemical properties of biomass were changed by the liquid catalyst in the pretreatment zone. During the ammonia–mechanical pretreatment process, the twin-screw extruder strengthened the interaction between biomass and aqueous ammonia by the twin-screw extruder. Wheat straw changed the physical properties, such as specific surface area, bulk density, and specific porosity in the deconstruction zone (Section 1) and the separation of cellulose fibers by aqueous ammonia in the pretreatment zone (Section 2). Because of friction heat generation, the extruder does not need an external heat source, and the operating temperature was maintained at about 373 K, which not only lessens energy

consumption and operating costs but also prevents lignin oxidation and carbohydrate degradation [28,29].

The compositional analysis of pretreatment residue under different conditions was used to estimate the effect of ammonia–mechanical pretreatment (Table 1). The delignification rate was significantly affected by the aqueous ammonia concentration and liquid–solid ratio. The delignification rate was 37.36 wt% when the aqueous ammonia concentration was 5% *w/w*, while it enhanced to 53.81 wt% when the aqueous ammonia concentration increased to 25% *w/w* (Table 1, entries 2 and 10). Similarly, the delignification rate was increased with the liquid–solid ratio (Table 1, entries 3 and 8). However, the holding time had little effect on the delignification (Table 1, entries 2 and 7). The synergy of the aqueous ammonia and twin-screw extruder provided a particularly effective method to remove the lignin, which broke the ester bond between the hemicellulose and lignin [30]. The recovered cellulose content was higher than that for hemicellulose, which was ascribed to deacetylation during pretreatment [31]. Under the optimal conditions (Table 1, entry 18, based on Box–Behnken design, *vide infra*), the recovery of cellulose and hemicellulose was 86.90% and 68.57%, respectively, and the delignification was 62.47%.

Table 1. Compositional analysis of wheat straw using ammonia–mechanical pretreatment.

Entry	X ₁ ^c	X ₂ ^d	X ₃ ^e	Solid Remain %	Cellulose %		Hemicellulose %		Lignin %	
					Content	Recovery	Content	Recovery	Content	Delignification
Raw	-	-	-	-	34.91	-	22.58	-	23.03	-
1 ^a	15	3:1	6	57.40	49.00	80.56	23.22	59.03	15.05	62.50
2 ^a	25	2:1	6	63.00	44.32	79.98	21.77	60.73	16.89	53.81
3 ^a	25	3:1	4	64.10	45.80	84.09	22.55	64.02	16.75	53.37
4 ^a	15	2:1	4	52.31	38.09	57.07	20.52	47.55	18.03	59.05
5 ^a	15	3:1	2	59.14	44.86	76.00	23.89	62.56	17.55	54.94
6 ^a	15	1:1	2	55.56	35.93	57.19	19.62	48.27	18.75	54.77
7 ^a	25	2:1	2	61.29	40.16	70.50	23.22	63.03	18.65	50.36
8 ^a	25	1:1	4	72.63	41.15	85.61	21.19	68.16	19.77	37.67
9 ^a	15	2:1	4	58.42	44.69	74.79	23.25	60.15	15.45	60.80
10 ^a	5	2:1	6	69.26	41.80	82.93	21.95	67.32	20.83	37.36
11 ^a	5	3:1	4	58.38	47.13	78.81	23.76	61.44	16.83	57.35
12 ^a	5	2:1	2	68.16	40.72	79.51	22.49	67.90	20.07	40.60
13 ^a	5	1:1	4	62.08	41.40	73.63	22.43	61.67	20.95	43.54
14 ^a	15	2:1	4	58.16	40.35	67.23	21.19	54.58	16.21	59.06
15 ^a	15	2:1	4	51.02	39.84	58.23	21.34	48.22	16.17	64.17
16 ^a	15	2:1	4	51.02	39.02	57.03	20.62	46.58	17.40	61.45
17 ^a	15	1:1	6	65.85	34.86	65.75	19.16	55.88	17.24	50.70
18 ^b	19	2.1:1	4.8	60.36	50.26	86.90	25.65	68.57	14.32	62.47

^a The pretreatment residue under BBD conditions. ^b The pretreatment residue under the optimal condition. ^c Aqueous ammonia concentration (*w/w*). ^d Liquid–solid ratio (*w/w*). ^e Holding time (h).

The conversion rate of carbohydrates was a crucial metric for assessing the efficacy of pretreatment. As shown in Figure 2, these values indicate that ammonia–mechanical pretreatment significantly enhanced the conversion of carbohydrates to monosaccharides. This was related to the removal of hemicellulose and a large amount of lignin from the wheat straw (Table 1). The lignin as a physical barrier can hinder the enzymatic hydrolysis of biomass, and removed lignin can reduce the unproductive adsorption with cellulase to improve enzymatic hydrolysis [32,33].

Box–Behnken design (BBD) was used to further investigate the effect of independent variables on response values and to optimize the cellulose and hemicellulose conversion (Table S2). The regression coefficient was significant (99%) due to the predicted second-order polynomial model, with the probability *p* value <0.01, and the probability of noise of cellulose and hemicellulose conversions was only 0.01% and 0.15%, respectively. The prominent F-values of cellulose and hemicellulose conversions were 25.70 and 12.72, re-

spectively. The lack of fit (LoF) of the center point experimental results was too insignificant ($p > 0.05$) to reflect the accuracy of the model, based on the coefficient of determination (R^2), 0.9706 and 0.9424 for cellulose and hemicellulose conversions. The polynomial model showed an excellent relationship with the experimental and predicted values. The chart of experimental results and model predictions is shown in Figure S2, which further verifies the adequacy of the model.

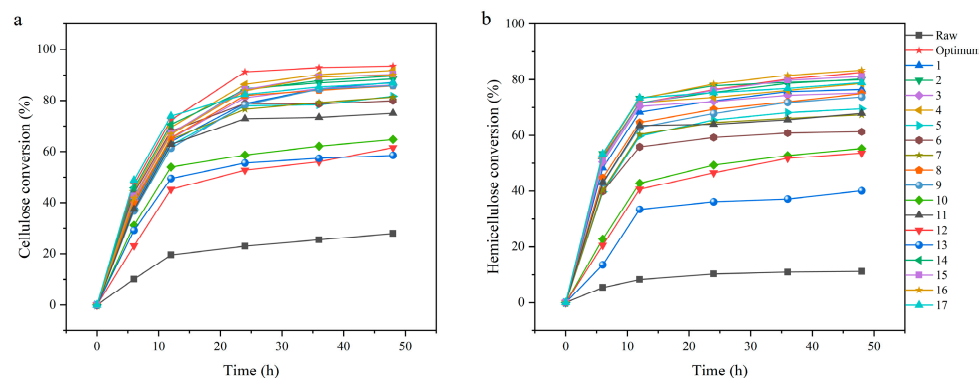


Figure 2. The curve of time–carbohydrate hydrolysis at pH 4.8 and 323.15 K. (a) Cellulose; (b) hemicellulose.

The influence of the cellulose conversion included aqueous ammonia concentration, liquid–solid ratio, and holding time, as shown in the 3D surface graph (Figure 3a–c). Cellulose conversion changed significantly ($p < 0.05$) with increased liquid–solid ratio and holding time, while the effect of aqueous ammonia concentration on the cellulose conversion was more pronounced ($p < 0.01$). The cellulose conversion increased first and then decreased when the aqueous ammonia concentration raised from 5 to 25% w/w (Figure 3a), indicating that high aqueous ammonia had adverse effects on the cellulose conversion. Within a certain range, there were positive effects on cellulose conversion from the interaction between aqueous ammonia concentration and holding time (Figure 3b). Compared to the interaction between ammonia concentration and liquid–solid ratio (Figure 3a), and the interaction between ammonia concentration and holding time (Figure 3b), the interaction of liquid–solid ratio and holding time showed less effect on the cellulose conversion, which was reflected in the relatively flat 3D surface graph (Figure 3c).

Meanwhile, the 3D response surface plot demonstrated the hemicellulose conversion of wheat straw by the interaction of independent variables (Figure 3d–f). Aqueous ammonia concentration was the most critical factor for the hemicellulose conversion of wheat straw ($p < 0.01$), followed by holding time and liquid–solid ratio level factors. To some extent, the hemicellulose conversion gradually increased with the aqueous ammonia concentration, and the liquid–solid ratio was enhanced (Figure 3d). Increased aqueous ammonia concentration extended the holding time, which increased the hemicellulose conversion through enhancing the disruption of the amorphous region (Figure 3e). The effect of holding time and liquid–solid ratio interaction on hemicellulose conversion was small, which can be observed from the response surface (Figure 3f).

In this study, we calculated the optimal conditions of cellulose and hemicellulose conversions by setting the partial derivatives of the second-order polynomial equation for their corresponding variables to zero. The optimal value of the cellulose and hemicellulose conversions predicted by the response surface methodology model was 92.45% and 83.39% at 19% w/w aqueous ammonia concentration with 2.1:1 w/w of liquid–solid ratio level for 4.80 h holding time of the ammonia–mechanical pretreatment conditions. Then, we performed the validation experiments and obtained the conversion of 93.47% and 82.61% for cellulose and hemicellulose, which was comparable to the predicted value and further indicated the accuracy and validity of the Box–Behnken design.

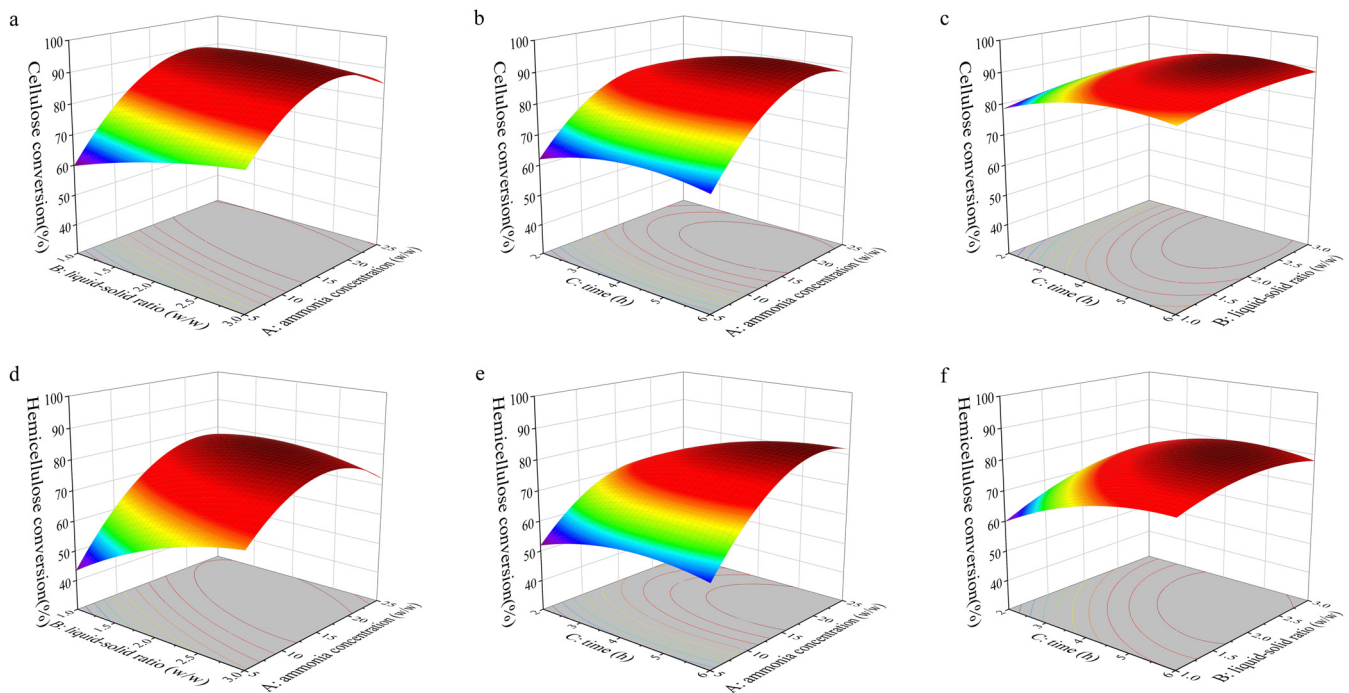


Figure 3. Effect of aqueous ammonia concentration, liquid–solid ratio and holding time on the conversion. (a–c) Cellulose conversion; (d–f) hemicellulose conversion.

3.2. L-Lactic Acid Fermentation

The formation of inhibitors was a critical criterion for the quality of pretreatment. According to HPLC analysis, furfural, 5-hydroxymethyl furfural, acetic acid, and formic acid are usually generated during the traditional pretreatment process and are not found in the present wheat straw hydrolysate (Table S3) [34]. These results suggested that the hydrolysate obtained via ammonia–mechanical pretreatment was suitable for fermentation. Furthermore, the utilization of xylose was critical to improving the appended value of integrated biorefineries [35]. Thus, an engineered bacterium strain with active pentose assimilation, *Thermoanaerobacter* sp. DH-217G, can provide the basis for efficient utilization of hexose and pentose of the hydrolysate as carbon sources for the fermentation to produce L-lactic acid.

Both mixtures of pure sugar and wheat straw hydrolysate as the carbon source for L-lactic acid fermentation are shown in Figure 4. As shown in Figure 4a, *Thermoanaerobacter* sp. DH-217G can utilize glucose and trigger the successful assimilation of xylose to L-lactic acid. The L-lactic acid was obtained within 58 h of sugar fermentation, and the productivity was 0.908 grams per gram of the mixture of pure sugars. At the end of fermentation, L-lactic acid was obtained at 85.32 g/L, with 1.87 g/L of total sugar residues (glucose, ~1.43 g/L; xylose, ~0.44 g/L). In addition, the chiral purity of L-lactic acid was measured as 99.5% using the Megazyme D-/L-lactic acid kit. A striking feature of lactic acid production by wheat straw hydrolysate relative to a mixture of pure sugars was the extended fermentation time up to 64 h (Figure 4b). L-lactic acid was obtained by 79.58 g/L with the productivity of 0.886 grams per gram of sugars, with only 1.78 g/L total sugar residues (glucose, ~1.68 g/L; xylose, ~0.10 g/L) at the end of fermentation. When comparing lactic acid fermentation with other reports, the *ulva* sp. fermentation using *Lactobacillus* sp. (0.85 grams per gram of sugars) [36] and the inedible starchy biomass fermentation using thermotolerant *Lactobacillus rhamnosus* DUT1908 (0.89 grams per gram of sugar) [37] showed that the hydrolysate obtained from the ammonia–mechanical pretreatment was suitable for L-lactic acid fermentation. In addition, the chiral purity of L-lactic acid was measured as 99.2%, which was due to the complexity of the wheat straw hydrolysate.

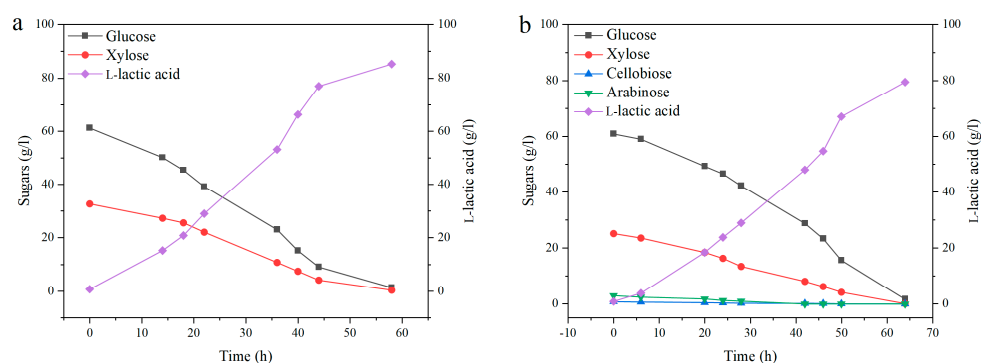


Figure 4. L-lactic acid product by *Thermoanaerobacter* sp. DH-217G at pH 6.8 and 328.15 K. (a) Mixture of pure sugars; (b) wheat straw hydrolysate.

3.3. Mass Balance under the Optimal Reaction Condition

Based on the Box–Behnken design, we studied the feasibility of the ammonia–mechanical pretreatment process through the holistic mass balance under optimal conditions. First, 10 kg wheat straw was treated with a twin-screw extruder, 19% *w/w* aqueous ammonia concentration, liquid–solid ratio 2.1:1 *w/w*, and heat preservation for 4.8 h. After pretreatment, the black liquor and pretreatment residue was separated. The pretreatment residue (60.36 wt%) was washed for enzymatic hydrolysis, and the sugar yield was about 89.37% based on the sugar in the pretreatment residue. The aqueous ammonia recovered under evaporation from the black liquor and filtrate, and the lignin recovered by spray drying. The recovery rate of aqueous ammonia was about 70% due to some aqueous ammonia consumed by the chemical reaction between aqueous ammonia and lignin (*vide infra*). As shown in Figure 5, the results show that 4.920 kg of calcium L-lactic acid was produced from 10 kg of dry wheat straw, equivalent to 4.062 kg of L-lactic acid. The final lactic acid yield was about 88.59% based on the hydrolysate and 63.03% based on the total sugar in the wheat straw.

3.4. Microstructure of Pretreatment Residue

The microstructures of the wheat straw and pretreatment residues were studied using SEM and X-ray diffraction (Figures S3 and S4). The untreated wheat straw had a dense and well-arranged surface structure. This structure acts as a barrier to enzymes and reduces their accessibility by preventing cellulase from entering the straw. After pretreatment, the complete and orderly appearance of the wheat straw was disrupted and created a loose and rough structure with a large distribution of pores. Different levels removed of lignin and hemicellulose led to the gradual exposure of cellulose. The results showed that the destruction of the lignin physical barrier and exposure to cellulose increased the accessibility of cellulose. In addition, the crystallinity of wheat straw was changed from 47.69% to 53.57% (Table S4), mainly due to the degradation of a minor amount of amorphous hemicellulose and a large amount of lignin during the pretreatment process (Table 1).

3.5. Structural Characterization of Extracted Lignin

3.5.1. FTIR and Ultimate Analysis

The lignin samples were investigated by FTIR (Figure 6). Milled wood lignin (MWL) is close to its primitive status and commonly exhibits much smaller structural variations. Thus, MWL derived from the wheat straw was selected for comparison. The -OH stretching vibration signal was at 3381 cm^{-1} , and the C-H stretching vibration signal was at 2927 and 2842 cm^{-1} , which were the feature absorption peaks of lignin [38]. Meanwhile, the aromatic ring vibration (1598 and 1514 cm^{-1}), the guaiacyl (1252 cm^{-1}), the C-H deformation vibration connected to fragrant (1461 cm^{-1}), and the syringyl (1329 and 1130 cm^{-1}) were observed in the lignin samples [39]. The indicated lignin samples were representative of HGS lignin. Compared with MWL, P-lignin had a weaker peak intensity at 830 cm^{-1} (β -1,4-glycosidic

bond in cellulose) and 1040 cm^{-1} (C-O-H stretching of primary and secondary alcohols of cellulose). In addition, there was no peak at $1740\text{--}1735\text{ cm}^{-1}$ (the ester group of acetyl and glyoxylate of hemicellulose). The chemical bonds between carbohydrates and lignin were broken after ammonia–mechanical pretreatment. The disappearance of the signal (C=O) at 1702 cm^{-1} was probably due to the reduction of aqueous ammonia. The absorbance of P-lignin has a new peak at 1687 cm^{-1} (the signal of amido bond), which suggests that lignin grafted with nitrogen during the ammonia–mechanical pretreatment, which was further validated by ultimate analysis (Table S5) and 2D HSQC NMR (vide infra).

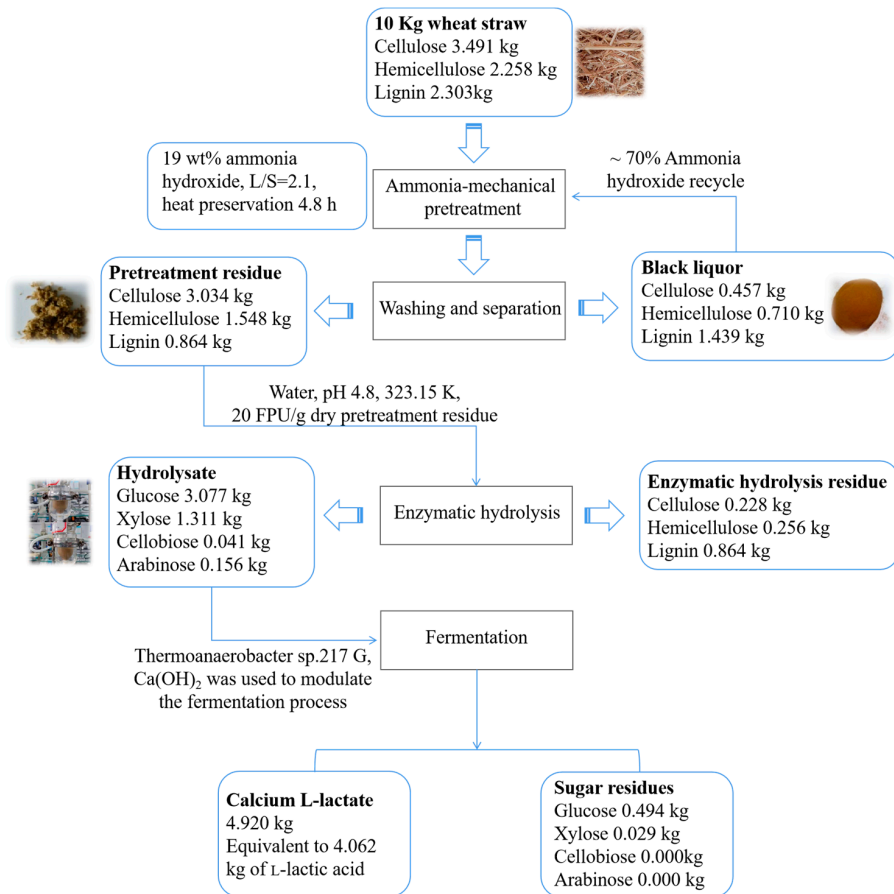


Figure 5. Mass balance of ammonia–mechanical pretreatment, enzymatic hydrolysis and fermentation.

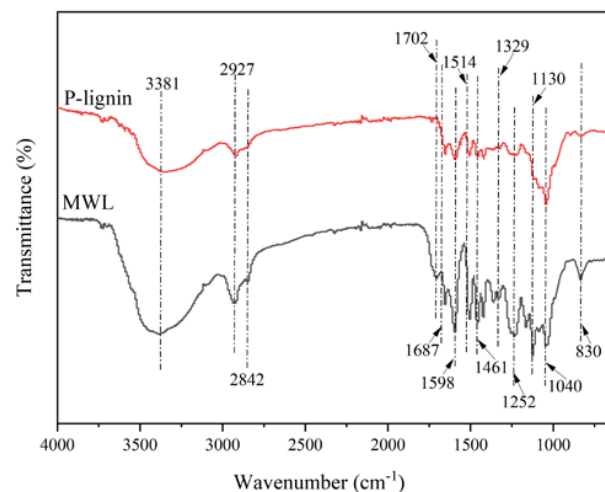


Figure 6. FTIR spectra of MWL and P-lignin (extracted at optimal pretreatment conditions).

3.5.2. Two-dimensional ^1H - ^{13}C HSQC NMR Analysis

The structure of lignin was further studied by 2D-HSQC NMR analysis (Figure 7), which included the side-chain ($\delta_{\text{C}}/\delta_{\text{H}}$ 50–90/2.5–6.0 ppm) and the aromatic regions ($\delta_{\text{C}}/\delta_{\text{H}}$ 90–160/6.0–8.0 ppm) (Table S6). The content of β -O-4 aryl ether linkages (A) and C-H in phenylcoumaran substructures (B) was detected in the side-chain regions [40]. The P-lignin was confirmed to be GSH lignin due to the signals of guaiacyl (G), syringyl (S), p-hydroxy phenyl (H), triclin (T), and ferulate (FA), which were all observed in the aromatic ring regions. The most interesting feature was that the ester bond-linked ferulic acid with grafted nitrogen, ferulamide (FAM₆, $\delta_{\text{C}}/\delta_{\text{H}}$ 123.1/7.20), was detected in P-lignin, which manifested the ammonolysis of the lignin that occurred during the pretreatment [41]. Based on the ultimate analysis, the nitrogen of the P-lignin was increased 12.81 times compared to the MWL. By contrast, the signal of FA _{α} ($\delta_{\text{C}}/\delta_{\text{H}}$ 145.2/7.58) vanished after pretreatment, which was mainly due to the reduction of the $\alpha=\beta$ double bond caused by the reducibility of the aqueous ammonia. Furthermore, the triclin was unstable and was reflected in the disappearance of the T₆ ($\delta_{\text{C}}/\delta_{\text{H}}$ 98.9/6.23) and T₈ ($\delta_{\text{C}}/\delta_{\text{H}}$ 94.2/6.60) signals, which may be dissolved and destroyed during the ammonia-mechanical pretreatment [42]. Lastly, some β -O-4 aryl ether linkages were cleaved by alkali catalysis of the aqueous ammonia, which was reflected in the signal of A _{α} ($\delta_{\text{C}}/\delta_{\text{H}}$ 71.6/4.88) [43]. In addition, the S/G/H ratio of MWL and P-lignin was 55/44/1 and 50/48/2, respectively. The S/G ratio of lignin decreased from 1.27 to 1.06 after ammonia-mechanical pretreatment, indicating that demethylation may occur during the process.

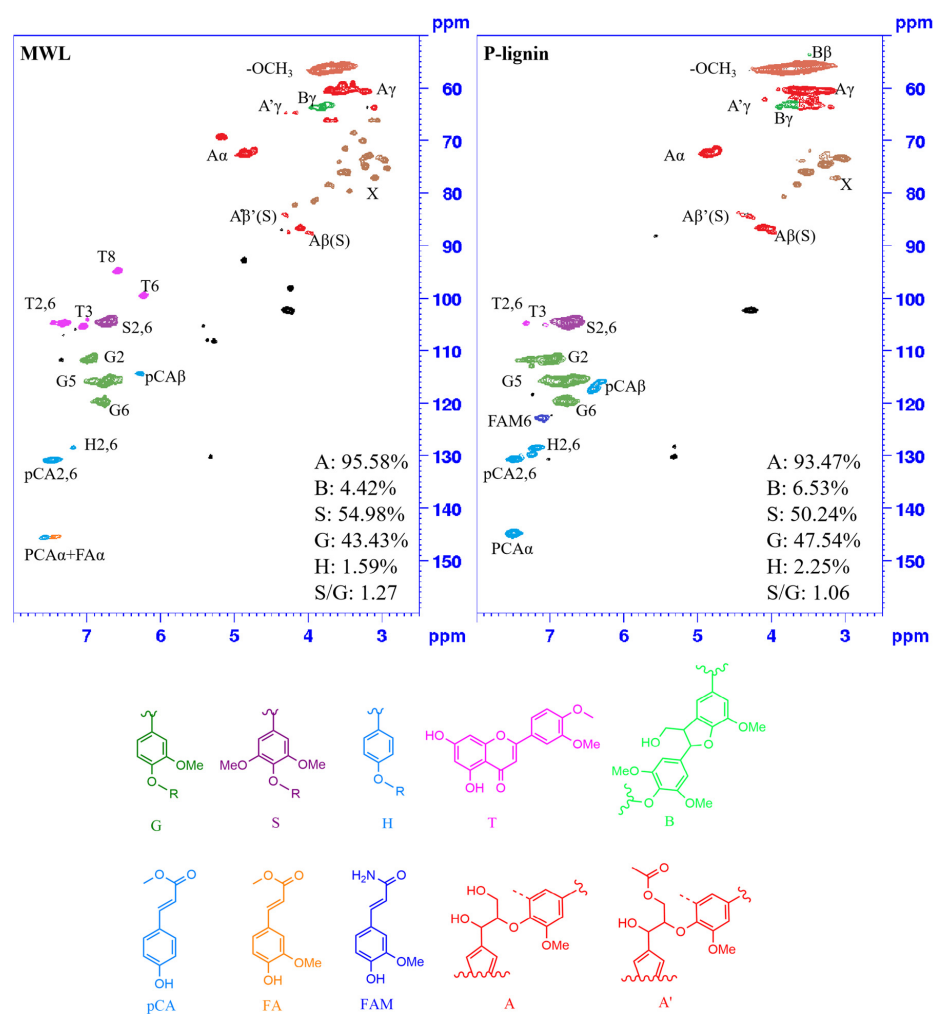


Figure 7. Two-dimensional HSQC NMR spectra of MWL and P-lignin (extracted at optimal pretreatment conditions). Signals are depicted in Table S6.

3.5.3. The Radical Scavenging Activity of Lignin

The radical scavenging activity of lignin can reflect the antioxidant activity of lignin. The results of the radical scavenging activity of P-lignin and MWL were determined by the DPPH kit and showed that P-lignin (61.12%) was higher than MWL (38.99%). Co-production of radical scavenging activity lignin becomes another advantage of the ammonia–mechanical pretreatment system, which provides the potential for further downstream high value-added applications, such as it can act as an antioxidant additive for films, polymers, and other [44].

4. Conclusions

In short, an efficient and mild ammonia–mechanical pretreatment system to overcome the problems of saline wastewater brought on by the traditional alkali process is presented. Delignification of 62.47% and total sugar yield of 89.37% based on the sugar in the pretreatment residue (corresponding to 71.14% based on the raw wheat straw) was achieved under the optimal condition. With the aid of the developed extrusion equipment, the energy consumption was greatly reduced compared with the traditional cooking method. Lastly, 79.58 g/L of L-lactic acid with a yield of 88.59% and optical purity of 99.2% can be obtained using the wheat straw hydrolysate.

Supplementary Materials: The following supporting information can be downloaded at: <https://www.mdpi.com/article/10.3390/fermentation9020177/s1>, Figure S1: Twin-screw element structure diagram; Figure S2: Predicted vs. experimental of conversion. (a) Cellulose; (b) hemicellulose; Figure S3: SEM micrographs of wheat straw and pretreatment residue (at optimal pretreatment conditions). (a,b) Wheat straw, (c,d) pretreatment residue; Figure S4: XRD of wheat straw and pretreatment residue (at optimal pretreatment conditions); Table S1: Box–Behnken design (BBD) for optimization of process parameters affecting cellulose conversion ($Y_{\text{Glucose-end}}$) and hemicellulose conversion ($Y_{\text{Xylose-end}}$) during ammonia–mechanical pretreatment of wheat straw; Table S2: ANOVA table of linear, quadratic and interactive terms of ammonia–mechanical pretreatment process variables on responses (F-value); Table S3: Composition of wheat straw enzymatic hydrolysate used for lactic acid fermentation; Table S4: The crystallinity index of wheat straw and pretreatment residue (at optimal pretreatment conditions); Table S5: Ultimate analysis of MWL and P-lignin (extracted at optimal pretreatment conditions); Table S6: Assignment of main lignin ^{13}C - ^1H cross-signals in the HSQC spectra.

Author Contributions: Y.C. (Yulian Cao): Conceptualization, methodology, formal analysis, writing—original draft. H.L.: methodology, investigation, data curation. J.S.: methodology, data curation. B.S.: methodology, data curation. Y.C. (YanJun Chen): data curation, supervision. L.J.: supervision, writing—review and editing. X.J.: supervision, writing—review and editing. J.W.: supervision, writing—review and editing. C.Z.: project administration, funding acquisition, writing—review and editing, supervision. H.Y.: resources, supervision, conceptualization. All authors have read and agreed to the published version of the manuscript.

Funding: This work was supported by grants from the National Natural Science Foundation of China (grant no. 22178170), Six talent peaks project in Jiangsu Province (SWYY-016), the Foundation (no. GZKF202222) of State Key Laboratory of Biobased Material and Green Papermaking, Qilu University of Technology, Shandong Academy of Sciences, and the Key Research and Development Plan of Jiangsu Province (grant no. BE2020712).

Institutional Review Board Statement: Not applicable.

Informed Consent Statement: Not applicable.

Data Availability Statement: Not applicable.

Conflicts of Interest: The authors declare no conflict of interest.

References

1. Castillo Martinez, F.A.; Balciunas, E.M.; Salgado, J.M.; Domínguez González, J.M.; Converti, A.; de Souza Oliveira, R.P. Lactic acid properties, applications and production: A Review. *Trends Food Sci. Technol.* **2013**, *30*, 70–83. [[CrossRef](#)]
2. Yankov, D. Fermentative lactic acid production from lignocellulosic feedstocks: From source to purified product. *Front. Chem.* **2022**, *10*, 823005. [[CrossRef](#)] [[PubMed](#)]
3. Lin, H.-T.V.; Huang, M.Y.; Kao, T.Y.; Lu, W.J.; Lin, H.J.; Pan, C.L. Production of lactic acid from seaweed hydrolysates via lactic acid bacteria fermentation. *Fermentation* **2020**, *6*, 37. [[CrossRef](#)]
4. Abdel-Rahman, M.A.; Tashiro, Y.; Sonomoto, K. Lactic acid production from lignocellulose-derived sugars using lactic acid bacteria: Overview and Limits. *J. Biotechnol.* **2011**, *156*, 286–301. [[CrossRef](#)] [[PubMed](#)]
5. Kim, J.; Kim, Y.-M.; Lebaka, V.R.; Wee, Y.J. Lactic acid for green chemical industry: Recent advances in and future prospects for production technology, recovery, and applications. *Fermentation* **2022**, *8*, 609. [[CrossRef](#)]
6. Raj, T.; Chandrasekhar, K.; Naresh Kumar, A.; Kim, S.H. Lignocellulosic biomass as renewable feedstock for biodegradable and recyclable plastics production: A sustainable approach. *Renew. Sustain. Energy Rev.* **2022**, *158*, 112130. [[CrossRef](#)]
7. Mankar, A.R.; Pandey, A.; Modak, A.; Pant, K.K. Pretreatment of lignocellulosic biomass: A review on recent advances. *Bioresour. Technol.* **2021**, *334*, 125235. [[CrossRef](#)] [[PubMed](#)]
8. Faiz Norrrahim, M.N.; Ilyas, R.A.; Nurazzi, N.M.; Asmal Rani, M.S.; Nur Atikah, M.S.; Shazleen, S.S. Chemical pretreatment of lignocellulosic biomass for the production of bioproducts: An overview. *Appl. Sci. Eng. Prog.* **2021**, *14*, 588–605. [[CrossRef](#)]
9. Jose, D.; Kitiborwornkul, N.; Sriariyanun, M.; Keerthi, K. A review on chemical pretreatment methods of lignocellulosic biomass: Recent advances and progress. *Appl. Sci. Eng. Prog.* **2022**, *15*, 6210. [[CrossRef](#)]
10. Kucharska, K.; Rybarczyk, P.; Hołowacz, I.; Łukajtis, R.; Glinka, M.; Kamiński, M. Pretreatment of lignocellulosic materials as substrates for fermentation processes. *Molecules* **2018**, *23*, 2937. [[CrossRef](#)] [[PubMed](#)]
11. Kim, J.S.; Lee, Y.Y.; Kim, T.H. A review on alkaline pretreatment technology for bioconversion of lignocellulosic biomass. *Bioresour. Technol.* **2016**, *199*, 42–48. [[CrossRef](#)] [[PubMed](#)]
12. Tang, C.; Shan, J.; Chen, Y.; Zhong, L.; Shen, T.; Zhu, C.; Ying, H. Organic amine catalytic organosolv pretreatment of corn stover for enzymatic saccharification and high-quality lignin. *Bioresour. Technol.* **2017**, *232*, 222–228. [[CrossRef](#)] [[PubMed](#)]
13. Zhong, L.; Zhang, X.; Tang, C.; Chen, Y.; Shen, T.; Zhu, C.; Ying, H. Hydrazine hydrate and organosolv synergetic pretreatment of corn stover to enhance enzymatic saccharification and co-production of high-quality antioxidant lignin. *Bioresour. Technol.* **2018**, *268*, 677–683. [[CrossRef](#)] [[PubMed](#)]
14. Li, X.; Kim, T.H. Low-liquid pretreatment of corn stover with aqueous ammonia. *Bioresour. Technol.* **2011**, *102*, 4779–4786. [[CrossRef](#)]
15. Le, T.D.T.; Nguyen Truong, V.P.; Ngo, M.T.T.; Kim, T.H.; Oh, K.K. Pretreatment of corn stover using an extremely low-liquid ammonia (ELLA) method for the effective utilization of sugars in simultaneous saccharification and fermentation (SSF) of ethanol. *Fermentation* **2021**, *7*, 191. [[CrossRef](#)]
16. Lau, M.W.; Gunawan, C.; Dale, B.E. The impacts of pretreatment on the fermentability of pretreated lignocellulosic biomass: A comparative evaluation between ammonia fiber expansion and dilute acid pretreatment. *Biotechnol. Biofuels* **2009**, *2*, 30. [[CrossRef](#)]
17. Duque, A.; Manzanares, P.; Ballesteros, M. Extrusion as a pretreatment for lignocellulosic biomass: Fundamentals and applications. *Renew. Energy* **2017**, *114*, 1427–1441. [[CrossRef](#)]
18. José, Á.H.M.; Moura, E.A.B.; Rodrigues Jr, D.; Kleingesinds, E.K.; Rodrigues, R.C.L.B. A residue-free and effective corncob extrusion pretreatment for the enhancement of high solids loading enzymatic hydrolysis to produce sugars. *Ind. Crops Prod.* **2022**, *188*, 115655. [[CrossRef](#)]
19. Phojaroen, J.; Jiradechakorn, T.; Kirdponpattara, S.; Sriariyanun, M.; Junthip, J.; Chuetor, S. Performance evaluation of combined hydrothermal-mechanical pretreatment of lignocellulosic biomass for enzymatic enhancement. *Polymers* **2022**, *14*, 2313. [[CrossRef](#)]
20. Areepak, C.; Jiradechakorn, T.; Chuetor, S.; Phalakornkule, C.; Sriariyanun, M.; Raita, M.; Champreda, V.; Laosiripojana, N. Improvement of lignocellulosic pretreatment efficiency by combined chemo—Mechanical pretreatment for energy consumption reduction and biofuel production. *Renew. Energy* **2022**, *182*, 1094–1102. [[CrossRef](#)]
21. Chuetor, S.; Ruiz, T.; Barakat, A.; Laosiripojana, N.; Champreda, V.; Sriariyanun, M. Evaluation of rice straw biopowder from alkaline-mechanical pretreatment by hydro-textural approach. *Bioresour. Technol.* **2021**, *323*, 124619. [[CrossRef](#)] [[PubMed](#)]
22. Liu, C.; van der Heide, E.; Wang, H.; Li, B.; Yu, G.; Mu, X. Alkaline twin-screw extrusion pretreatment for fermentable sugar production. *Biotechnol. Biofuels* **2013**, *6*, 97. [[CrossRef](#)] [[PubMed](#)]
23. Choi, C.H.; Oh, K.K. Application of a continuous twin screw-driven process for dilute acid pretreatment of rape straw. *Bioresour. Technol.* **2012**, *110*, 349–354. [[CrossRef](#)] [[PubMed](#)]
24. Björkman, A. Studies on the finely divided wood. Part I. Extraction of lignin with neutral solvents. *Svensk Papperstid.* **1956**, *59*, 477–485.
25. He, M.K.; He, Y.L.; Li, Z.Q.; Zhao, L.N.; Zhang, S.Q.; Liu, H.M.; Qin, Z. Structural characterization of lignin and lignin-carbohydrate complex (LCC) of sesame hull. *Int. J. Biol. Macromol.* **2022**, *209*, 258–267. [[CrossRef](#)] [[PubMed](#)]
26. Sluiter, A.; Hames, B.; Ruiz, R.; Scarlata, C.; Sluiter, J.; Templeton, D.; Crocker, D. Determination of structural carbohydrates and lignin in biomass. *Natl. Renew. Energy Lab.* **2008**, *1617*, 1–16.
27. Tang, C.; Chen, Y.; Liu, J.; Shen, T.; Cao, Z.; Shan, J.; Zhu, C.; Ying, H. Sustainable biobutanol production using alkali-catalyzed organosolv pretreated cornstalks. *Ind. Crops Prod.* **2017**, *95*, 383–392. [[CrossRef](#)]

28. Yoo, J.; Alavi, S.; Vadlani, P.; Amanor-Boadu, V. Thermo-mechanical extrusion pretreatment for conversion of soybean hulls to fermentable sugars. *Bioresour. Technol.* **2011**, *102*, 7583–7590. [[CrossRef](#)]
29. Zheng, J.; Rehmann, L. Extrusion pretreatment of lignocellulosic biomass: A review. *Int. J. Mol. Sci.* **2014**, *15*, 18967–18984. [[CrossRef](#)]
30. Li, G.; Sun, Y.; Guo, W.; Yuan, L. Comparison of various pretreatment strategies and their effect on chemistry and structure of sugar beet pulp. *J. Clean. Prod.* **2018**, *181*, 217–223. [[CrossRef](#)]
31. De Assis Castro, R.C.; Fonseca, B.G.; dos Santos, H.T.L.; Ferreira, I.S.; Mussatto, S.I.; Roberto, I.C. Alkaline deacetylation as a strategy to improve sugars recovery and ethanol production from rice straw hemicellulose and cellulose. *Ind. Crops Prod.* **2017**, *106*, 65–73. [[CrossRef](#)]
32. Alawad, I.; Ibrahim, H. Pretreatment of agricultural lignocellulosic biomass for fermentable sugar: Opportunities, challenges, and future trends. *Biomass Convers. Biorefinery* **2022**, accepted. [[CrossRef](#)]
33. Usmani, Z.; Sharma, M.; Awasthi, A.K.; Lukk, T.; Tuohy, M.G.; Gong, L.; Nguyen-Tri, P.; Goddard, A.D.; Bill, R.M.; Nayak, S.C.; et al. Lignocellulosic biorefineries: The current state of challenges and strategies for efficient commercialization. *Renew. Sustain. Energy Rev.* **2021**, *148*, 111258. [[CrossRef](#)]
34. Halder, D.; Purkait, M.K. A review on the environment-friendly emerging techniques for pretreatment of lignocellulosic biomass: Mechanistic insight and advancements. *Chemosphere* **2021**, *264*, 128523. [[CrossRef](#)] [[PubMed](#)]
35. Narisetty, V.; Cox, R.; Bommareddy, R.; Agrawal, D.; Ahmad, E.; Pant, K.K.; Chandel, A.K.; Bhatia, S.K.; Kumar, D.; Binod, P.; et al. Valorisation of xylose to renewable fuels and chemicals, an essential step in augmenting the commercial viability of lignocellulosic biorefineries. *Sustain. Energy Fuels* **2022**, *6*, 29–65. [[CrossRef](#)]
36. Nagarajan, D.; Oktarina, N.; Chen, P.T.; Chen, C.Y.; Lee, D.J.; Chang, J.S. Fermentative lactic acid production from seaweed hydrolysate using *Lactobacillus* sp. and *Weissella* sp. *Bioresour. Technol.* **2022**, *344*, 126166. [[CrossRef](#)]
37. Sun, Y.; Liu, H.; Yang, Y.; Zhou, X.; Xiu, Z. High-efficient L-lactic acid production from inedible starchy biomass by one-step open fermentation using thermotolerant lactobacillus rhamnosus dut1908. *Bioprocess Biosyst. Eng.* **2021**, *44*, 1935–1941. [[CrossRef](#)]
38. Deng, Y.; Qiu, Y.; Yao, Y.; Ayiania, M.; Davaritouchae, M. Weak-base pretreatment to increase biomethane production from wheat straw. *Environ. Sci. Pollut. Res.* **2020**, *27*, 37989–38003. [[CrossRef](#)]
39. Qiao, X.; Zhao, C.; Shao, Q.; Hassan, M. Structural characterization of corn stover lignin after hydrogen peroxide presoaking prior to ammonia fiber expansion pretreatment. *Energy Fuels* **2018**, *32*, 6022–6030. [[CrossRef](#)]
40. Zhao, C.; Qiao, X.; Shao, Q.; Hassan, M.; Ma, Z.; Yao, L. Synergistic effect of hydrogen peroxide and ammonia on lignin. *Ind. Crops Prod.* **2020**, *146*, 112177. [[CrossRef](#)]
41. Mittal, A.; Katahira, R.; Donohoe, B.S.; Pattathil, S.; Kandemkavil, S.; Reed, M.L.; Bidy, M.J.; Beckham, G.T. Ammonia pretreatment of corn stover enables facile lignin extraction. *ACS Sustain. Chem. Eng.* **2017**, *5*, 2544–2561. [[CrossRef](#)]
42. Miyamoto, T.; Mihashi, A.; Yamamura, M.; Tobimatsu, Y.; Suzuki, S.; Takada, R.; Kobayashi, Y.; Umezawa, T. Comparative analysis of lignin chemical structures of sugarcane bagasse pretreated by alkaline, hydrothermal, and dilute sulfuric acid methods. *Ind. Crops Prod.* **2018**, *121*, 124–131. [[CrossRef](#)]
43. Zhang, L.; Xu, Z.; Cort, J.R.; Vuorinen, T.; Yang, B. Flowthrough pretreatment of softwood under water-only and alkali conditions. *Energy Fuels* **2020**, *34*, 16310–16319. [[CrossRef](#)]
44. Lu, X.; Gu, X.; Shi, Y. A review on lignin antioxidants: Their sources, isolations, antioxidant activities and various applications. *Int. J. Biol. Macromol.* **2022**, *210*, 716–741. [[CrossRef](#)]

Disclaimer/Publisher’s Note: The statements, opinions and data contained in all publications are solely those of the individual author(s) and contributor(s) and not of MDPI and/or the editor(s). MDPI and/or the editor(s) disclaim responsibility for any injury to people or property resulting from any ideas, methods, instructions or products referred to in the content.